

# LightCode: Compiling LLM Inference for Photonic-Electronic Systems

Ryan Tomich,<sup>1</sup> Zhizhen Zhong,<sup>1</sup> and Dirk Englund<sup>1</sup>  
*Research Laboratory of Electronics, Massachusetts Institute of Technology*

(\*Electronic mail: rjtomich@mit.edu)

(Dated: 23 September 2025)

The growing demand for low-latency, energy-efficient inference in large language models (LLMs) has catalyzed interest in heterogeneous architectures. While GPUs remain dominant, they are poorly suited for integration with emerging domain-specific accelerators like the Photonic Tensor Units (PTUs), which offer low-power, high-throughput linear computation. This motivates hybrid compilation strategies that combine photonic and electronic resources. We present **LightCode**, a compiler framework and simulator for mapping LLM inference workloads across hybrid photonic–electronic systems. LightCode introduces the Stacked Graph, an intermediate representation that encodes multiple hardware-specific realizations of each tensor operation. Hardware assignment is formulated as a constrained subgraph selection problem optimized for latency or energy under parametric cost models. We evaluate LightCode on the prefill stage of GPT-2 and Llama-7B showing that under our workload and hardware assumptions, (i) Photonic hardware reduced energy by up to 50 % in our simulated workloads at maximum sequence length; (ii) multiplexing and assignment strategy yielded latency improvements exceeding 10 $\times$ ; and (iii) Optimizing for latency or energy resulted in distinct hardware mappings in our simulations. LightCode offers a module, foundational framework and simulator for compiling LLMs to emerging photonic accelerators. <sup>a</sup>

## I. INTRODUCTION

The development of large language models (LLMs) has led to increased model depth, width, and context length, driving extraordinary computational demands and making tensor operations a major performance bottleneck<sup>12</sup>. Broader deployment of LLMs in real-world applications have increased the overall volume of inference requests, making latency and energy efficiency critical design considerations<sup>156</sup>. While training requires enormous compute and memory resources, the inference stage—repeated billions of times in real-world deployments—dominates energy consumption and operational cost<sup>22,28</sup>. These demands drive heavy optimization of GPU-based inference pipelines within common frameworks like PyTorch<sup>5</sup> and TensorFlow<sup>3</sup>.

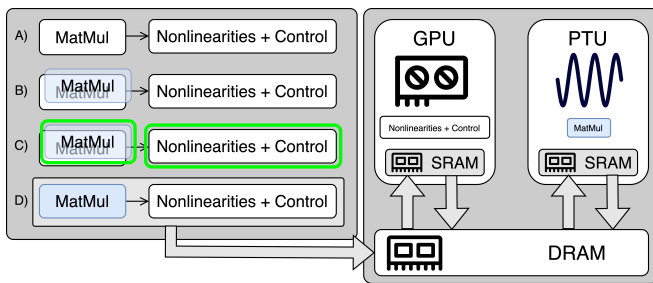


FIG. 1. Hybrid execution model with compiler-managed partitioning and scheduling across the GPU and Photonic Tensor Unit (PTU). A) Graph partitioning, B) Stack construction, C) Candidate selection, D) Scheduling.

## A. Machine Learning Compiler Infrastructure

ML compilers such as TensorFlow XLA<sup>13</sup>, Apache TVM<sup>8</sup>, Glow<sup>21</sup>, and MLIR<sup>14</sup> have become foundational tools for optimizing ML workloads. These compilers use IRs to apply a range of transformations, including operator fusion, layout optimization, constant folding, and hardware-aware scheduling. While these compilers target general-purpose hardware, the slowing of Moore’s Law has spurred growing interest in specialized accelerators that promise higher efficiency for domain-specific operations, such as tensor products<sup>11</sup>.

## B. Photonic Computing for ML Acceleration

Large-scale transformers spend > 95 % of their time and energy in dense matrix–vector or matrix–matrix multiples of width 1k–16k. Recent silicon-photonic tensor cores can execute those linear layers at <1 pJ per MAC and > 10 TOPS mm<sup>-2</sup>.<sup>9</sup> A time/space-multiplexed 2  $\times$  2 coherent X-bar operated at 20 GBd and 16- $\lambda$  WDM demonstrates 0.2 pJ MAC<sup>-1</sup> (0.8 TOPS on 0.04 mm<sup>2</sup>). An in-memory broadcast-and-weight microring array reaches 7.3 TOPS mm<sup>-2</sup> and the same 0.2 pJ MAC<sup>-1</sup> at 25 Gb s<sup>-1</sup>.<sup>29</sup> Survey data across >20 tape-outs place the median integrated MZI mesh at 0.3–3 pJ MAC<sup>-1</sup> with effective 6-bit linear precision.<sup>25</sup>

However, photonics is not a stand-alone compute platform for LLMs. A primary limitation is data-converter overhead: a single 6 GS s<sup>-1</sup> 8-bit ADC/DAC pair dissipates 25–80 fJ per sample, and in full-system models, cross-domain conversion and DRAM traffic often dominate the energy budget—exceeding photonic compute energy by 10 $\times$ .<sup>2</sup> Additionally, there exists an analog accuracy ceiling: fabrication variability and shot-noise limit the practical dynamic range to approximately 6 ENOB, with experimental studies reporting up to 15 % accuracy loss when such non-idealities are not prop-

<sup>a</sup>The following article has been submitted to *APL Photonics*. After it is published, it will be found at [Link](#).

erly compensated.<sup>10</sup> Furthermore, essential nonlinear operations such as activation functions, normalization, attention indexing, and control logic remain electronic, forcing every optical output to be converted back into the electrical domain.

Consequently, heterogeneous pipelines are currently a widely considered deployment model where photonic cores act as domain-specific accelerators for the linear sub-graphs, with GPUs or ASICs handling the surrounding non-linear and control logic—a design philosophy adopted, for example, by the Albireo light-offloading prototype.<sup>23</sup>

### C. Heterogeneous Compilation and Workload Partitioning

These heterogeneous pipelines consisting of GPU’s and PTU’s require coordination via a compiler capable of reasoning across devices with differing Instruction Set Architectures (ISAs), performance characteristics, and energy trade-offs. Compiling for heterogeneous hardware has long been a focus in systems such as OpenCL<sup>24</sup>, SYCL, and CUDA, which abstract coordination across CPUs, GPUs, and custom accelerators. These approaches address challenges such as workload partitioning and task scheduling, but relatively few compilers incorporate PTUs as first-class compilation targets.

This paper introduces **LightCode**, a compiler optimization framework and hardware-aware simulator designed to address this challenge. LightCode explicitly incorporates photonic compute constraints into the compilation and scheduling pipeline, enabling multi-target LLM inference across photonic and classical hardware. It transforms model execution traces into computation graphs and formulates the hardware mapping problem as a subgraph selection problem. LightCode then optimizes a cost function by partitions computation graphs, constructs per-target operation stacks, and selects the lowest-cost hardware mapping under realistic throughput and energy models. The main contributions of this paper are:

- LightCode Framework: Compiler and simulator for hybrid photonic–electronic LLM inference.
- Stacked Graph IR: Novel IR for selecting and mapping ops to optimal hardware.
- Evaluation on LLMs: Simulated validation of improved time and energy efficiency on Transformer models.

## II. PROBLEM STATEMENT

We define the hybrid compilation problem for photonic–electronic LLM inference as follows.

### A. Workload Setup

Each model is lowered to a tensor-level dataflow graph  $G = (V, E)$  via the TVM–Relay compiler. Each node  $v \in V$  represents an operator  $v_{\text{op}}$  that consumes and produces one or

more tensors. Each edge  $(u, v) \in E$  corresponds to a data dependency and is weighted by  $s_{u,v}$ , the number of bits in the tensor transferred from  $u$  to  $v$ . The total number of multiply-accumulate (MAC) operations is determined by the input sequence length  $S$ . We define these graphs for 2 transformer based LLM’s shown in Table I.

TABLE I. LLM workloads. Batch size is one; KV-cache is empty (worst-case prefill throughput).

Model	Layers	$d$	Params	Stage	$S$
GPT-2 Small	12	768	117M	Prefill	$\{100k \mid k \in \mathbb{N}_0, 0 \leq k \leq 10\}$
Llama-7B	32	4096	6.7B	Prefill	$\{100k \mid k \in \mathbb{N}_0, 0 \leq k \leq 40\}$

### B. Hardware Model

To evaluate alternative mapping strategies, we develop a modular simulator for heterogeneous hardware. Each hardware target in  $\mathcal{H} = \{\text{GPU, PTU}\}$  is modeled as a set of parallel cores with defined *throughput* (instructions per unit time) and *energy cost* (joules per instruction). Data transfers are characterized by *bandwidths* (bits per unit time) and *energy efficiencies* (joules per bit). Hardware parameter’s can be found in Table II.

TABLE II. GPU<sup>1</sup>, PTU, and memory parameters used in simulation. Energy values are reported per operation or bit.

Parameter	Symbol	Value
Clock frequency	$f_{\text{GPU}}$	1.98 GHz
	$f_{\text{PTU}}$	9.7 GHz <sup>28</sup>
Energy per MAC	$E_{\text{GPU}}$	0.07 pJ <sup>28</sup>
	$E_{\text{PTU}}$	0.04 pJ <sup>17,28</sup>
Compute cores	$N_{\text{GPU}}$	144
	$N_{\text{PTU}}$	1
Parallelism	$W$	20
FLOPs per cycle per core	$F_{cc}^{\text{GPU}}$	433
Memory Width	$b_{\text{mem}}$	32 bits
Memory clock rate	$f_{\text{mem}}$	$6 \times 10^9$ Hz (assumed)
DRAM energy	$E_{\text{DRAM}}$	1 pJ/bit <sup>4</sup>
SRAM energy	$E_{\text{SRAM}}$	0.3 pJ/bit <sup>4</sup>
Local memory RW	$E_{\text{local}}$	1 pJ (assumed)
DAC energy	$E_{\text{DAC}}$	10 pJ/sample <sup>4</sup>
ADC energy	$E_{\text{ADC}}$	3.17 pJ/sample <sup>4</sup>
DAC/ADC latency	$\ell_{ij}$	10 ns <sup>7,16</sup>

### C. Cost Functions

Each core type is associated with a set of *translation functions* that map high-level tensor operations to hardware-level instruction sequences. This function captures the architectural nuances of each target platform, such as vector widths, specialized compute units (e.g., tensor cores, photonic multipliers), and scheduling constraints. By applying these mappings to the computational graph, we derive a deterministic cost model for execution time and energy over the entire

computation graph. Inter-core and memory transfers are also explicitly modeled, accounting for latency and energy overheads per bit. This includes DRAM reads and writes, HBM accesses, SRAM operations, and transfers involving on-chip local memory. Additionally, the framework incorporates the cost of digital-to-analog (DAC) and analog-to-digital (ADC) conversions for photonic data paths. Given an assignment  $\mathbf{x}$  on the computation graph of operations to hardware targets:

Latency mode

$$c_{\text{lat}}(\mathbf{x}) = \sum_{v \in V} t_{h(v)}(v) + \sum_{(u,v) \in E} \tau_{h(u),h(v)}(s_{u,v})$$

Energy mode

$$c_{\text{eng}}(\mathbf{x}) = \sum_{v \in V} e_{h(v)}(v) + \sum_{(u,v) \in E} \varepsilon_{h(u),h(v)}(s_{u,v})$$

where

$$\begin{aligned} t_{\text{GPU}}(v) &= \frac{v_{\text{op}}}{F_{cc} \cdot N_{\text{GPU}}} & (\text{GPU compute time}) \\ t_{\text{PTU}}(v) &= \frac{v_{\text{op}}}{W \cdot N_{\text{PTU}}} & (\text{PTU compute time}) \\ e_{h(v)} &= v_{\text{op}} \cdot E_h & (\text{Energy per op on device } h) \\ \tau_{ij}(s) &= \frac{s_{i,j}}{b_{\text{mem}} \cdot f_{\text{mem}}} & (\text{Transfer time}) \\ \varepsilon_{ij}(s) &= s_{i,j} \cdot E_{\text{local}} \cdot E_{\text{SRAM}} & (\text{Transfer energy}) \end{aligned} \quad (1)$$

### III. METHODOLOGY

#### A. Stacked Graph Intermediate Representation

Having established a framework for representing programs as computation graphs over tensor operations, along with a cost model based on hardware-specific arithmetic capabilities, we now introduce a novel IR designed to enable multi-target optimization: the **Stacked Graph**. The Stacked Graph extends the traditional computation graph by duplicating each operation node for every supported hardware target. Each duplicate represents a hardware-specific implementation of the same logical operation, capturing the unique performance characteristics (e.g., latency or energy) of that backend. These alternatives are grouped into *stacks*, where each stack corresponds to a single logical operation and contains multiple candidate implementations—one per target hardware. Edges between nodes in adjacent stacks model data dependencies, forming a complete bipartite subgraph for each pair of connected stacks. As before, each node carries a weight corresponding to the execution cost of its associated implementation on its target hardware and each edge has a weight that reflects the data transfer cost between pairs of hardware components. An example of the GPU-PTU stacked graph for the encoding in the transformer architecture is depicted in Figure 2.

Formally, the Stacked Graph transforms a computation graph of operations into a graph of stacks, each encapsulating

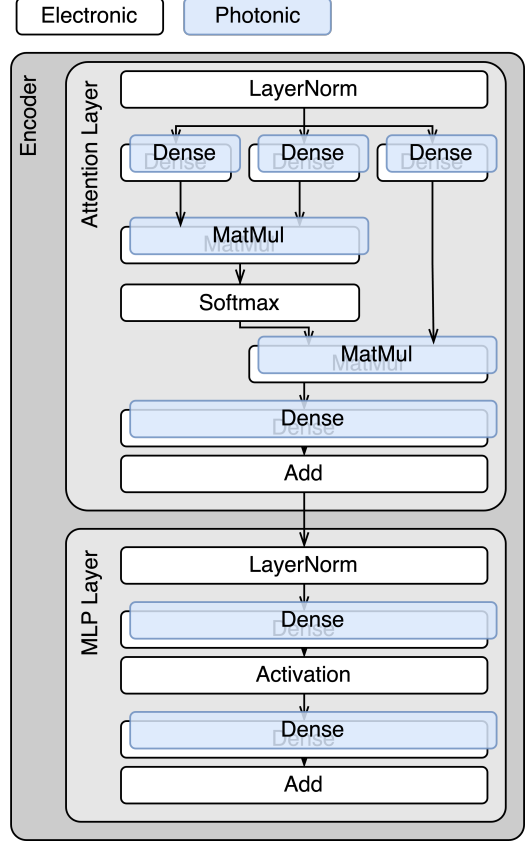


FIG. 2. Stacked Graph over a Transformer encoder block, illustrating logical operator grouping across hardware units. This block diagram presents a higher-level abstraction than the Relay IR presented in the Appendix Figure 8

a set of nodes for mutually exclusive implementation choices. That is, each operation  $v$  is assigned to a single node in each stack associated with one hardware target  $h \in \mathcal{H}$ :

$$x_{v,h} \in \{0, 1\} \text{ where } \sum_h x_{v,h} = 1.$$

This structure induces a natural optimization problem: select exactly one node from each stack and schedule it such that all inter-stack dependencies are respected and the total cost (execution + transfer) is minimized. This corresponds to a constrained subgraph selection problem over a hypergraph where the global objective is to construct a valid dataflow path with minimum cost. This optimization problem can be interpreted as a generalization of the *Group Steiner Tree* (GST) problem, in which each group corresponds to a stack and the goal is to select one node per group while minimizing the cost of connecting them. While GST is NP-hard in the general case, the repetitive and layered structure of transformer architecture<sup>26</sup> allows for algorithmic simplifications and scalable heuristics. In particular, the acyclic and modular topology of transformer computation graphs and the fact that it does not have adjacent linear operations enables graph partitioning strategies to reduce the search space and local greedy choices without sacrificing optimality.

## B. Optimization Pipeline

*a. Computation Graph* We begin by importing pre-trained model architectures from the Hugging Face model library<sup>27</sup> and lowering them to the TVM Relay IR<sup>19,20</sup>. This produces a computation graph that captures the dataflow dependencies between tensor operations, as defined in the preceding sections.

*b. Partition* At the tensor level, repeated layers in transformer-based LLMs induce isomorphic subgraphs in the computation graph. These graphs naturally expose articulation nodes—points whose removal increases the number of connected components—providing effective partitioning boundaries. Each component can then be optimized independently, reducing graph size and enabling optimization reuse across isomorphic subgraphs. This greatly improves tractability without compromising optimality, as articulation nodes in transformers under the Relay IR correspond to non-linear operations.

*c. Stack Construction* For each node in the partitioned graph, we enumerate all viable hardware-specific implementations supported by the available execution backends. Each node is replaced with a *stack* consisting of an implementation for each feasible hardware target. Each edge in the original computation graph becomes a set of edges between stacks, connecting all pairs of implementation between stacks. This yields the Stacked Graph IR that captures the all posable hardware mappings.

*d. Selection* We formulate the selection problem as a shortest-path search over the Stacked Graph. In the general case, we apply a modified Dijkstra’s algorithm to greedily extend shortest paths until a set of complete paths that includes one implementation per stack is identified. For transformer models, we exploit the fact that under the Relay IR, linear operations are not adjacent, which allows us to make locally optimal choices independently for each stack with multiple implementations. In this case, we restrict the subgraph to the target stack, its parent stacks, and its child stacks. The optimum for the target stack is selected by enumerating all options within that subgraph. Global optimality is preserved because linear operations are structurally separated, making each selection independent from the others. An example of a Relay IR partitioned and scheduled graph is presented in the Appendix under Figure 8.

*e. Scheduling* Once a single implementation has been selected for each stack, the Stacked Graph is flattened into a conventional computation graph by retaining only the chosen nodes and pruning all others. The partitioned subgraphs are then merged to reconstruct a unified, executable computation graph. We topologically sort the flattened computation graph to respect data dependencies and ensure valid execution ordering. Operations are scheduled in that topological order, taking into account backend-specific parallelism constraints and available compute resources. The final schedule maps operations to hardware units while honoring dependencies.

## IV. RESULTS

To evaluate hybrid execution performance, we analyze makespan and energy consumption under LightCode’s hardware mapping strategy (Fig.3). These results reflect a fixed photonic multiplexing factor of 20. We further explore the impact of multiplexing width on Llama-7B (Fig.4). To assess robustness, we conduct a sensitivity analysis over key hardware parameters from Table II, identifying the components most influential to system performance under both latency- and energy-driven objectives (Fig.5). Finally, Fig.6 disaggregates total energy by subsystem, quantifying the relative contributions of photonic, electronic, and memory elements across input sequence lengths.

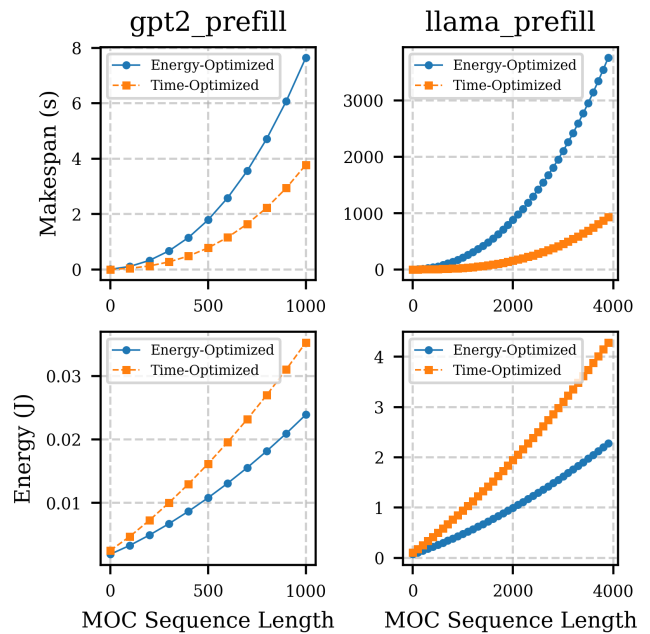


FIG. 3. Simulated makespan and energy usage during the prefill stage for Llama-7B and GPT-2 Small (PTU multiplexing = 20).

### A. Comparison to Prior Work

To validate the accuracy of LightCode’s energy modeling, we compare our results with those from Optical Transformers<sup>4</sup>, which estimates energy based on MAC operation counts and an experimentally obtained measurement for photonic dot-products.

For GPT-2 Small with a sequence length of 200 tokens, our simulation reports  $1.0988 \times 10^{11}$  MACs. Using a configuration that prioritizes photonic compute, total energy consumption is  $0.494 \times 10^{-2}$  J, with  $0.102 \times 10^{-2}$  J attributed to photonic cores—comparable to reported figures for GPT-2 Base in Optical Transformers<sup>4</sup>.

For Llama-7B at 400 tokens, the model performs  $1.204 \times 10^{13}$  MACs. Total energy consumption is 0.2209 J, with

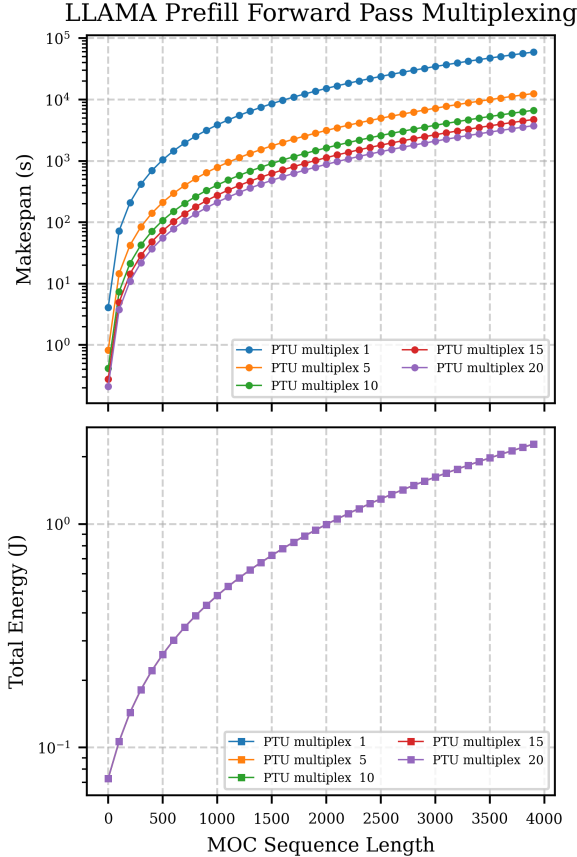


FIG. 4. Impact of PTU multiplexing factor on makespan and energy for Llama-7B during the prefill stage.

0.1074 J attributed to photonic units. These values are consistent with the estimates for the GPT-3 6.7B model in Optical Transformers<sup>4,18</sup>.

## B. Discussion

Under the stated workload, hardware, and cost model assumptions, Figure 3 show that the optimal hardware placement varies based on the performance metric. In our parameter sweep, lowest-latency configurations often keep linear ops on the GPU, while energy-optimized configurations offload them entirely to the PTU. This simulated result indicates photonic acceleration may not guarantee the optimal trade-off for every objective. Our simulators suggests photonic off-load yields large energy savings, but no latency improvements. The hardware mappings stayed consistent under varying hardware parameters shown in sensitivity analysis in Figure 5. Under the cost model and hardware assumptions, while increased multiplexing improves performance, Figure 4 shows gains start to diminish. We hypothesize that this is due to the assumed constraint that all multiplexed dot products must share a common operand (limiting reuse opportunities), and the observation that PTUs are typically data-bound rather

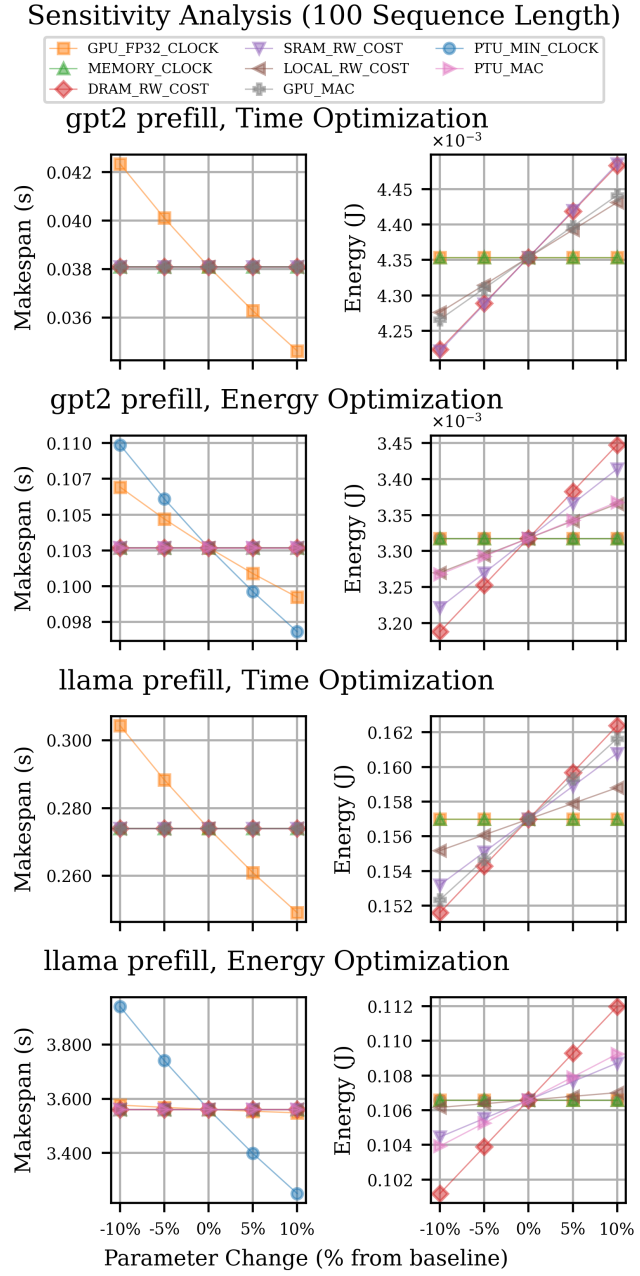


FIG. 5. Sensitivity of makespan and energy to hardware parameters for GPT-2 Small and Llama-7B (sequence length = 100) under time- and energy-optimized configurations.

than compute-bound, making memory throughput a critical bottleneck. Finally, Figure 6 reveals that under our assumptions, photonic dot products and data movement dominate energy consumption as sequence length grows.<sup>28</sup> This underscores the need for improving DAC/ADC efficiency and reducing conversion overheads to fully realize the potential of photonic accelerators.

These findings highlight the nuanced tradeoffs in deploying photonic accelerators for LLM inference. While photonic hardware can substantially reduce energy consumption for lin-

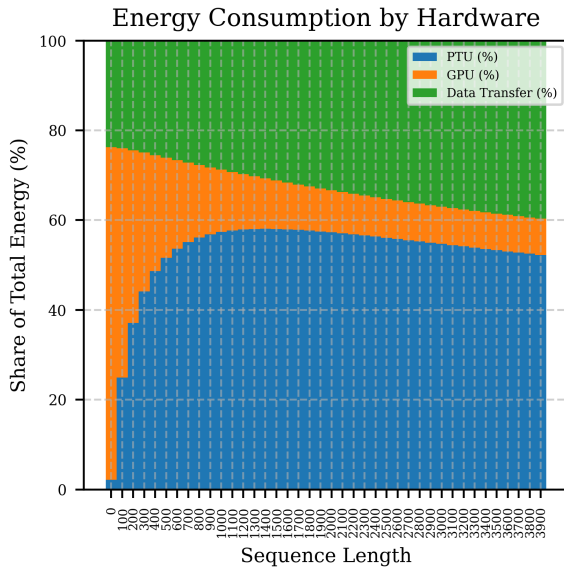


FIG. 6. Breakdown of energy consumption by component for Llama-7B across sequence lengths (PTU multiplexing = 20).

ear operations, its benefits are constrained by architectural and algorithmic bottlenecks such as memory bandwidth, operand reuse, and conversion overheads. The optimal hardware assignment strategy is workload- and objective-dependent: minimizing latency favors conventional GPUs, whereas minimizing energy favors aggressive photonic offloading. These findings validate the need for a flexible, workload-aware compiler infrastructure like LightCode capable of exploiting the complementary strengths of hybrid photonic-electronic systems for scalable, efficient LLM inference.

### C. Limitations

*a. Cost Model Simplification* The arithmetic hardware simulator used in LightCode provides a tractable alternative to cycle-accurate simulation (e.g., gem5), but does not model cache behavior, interrupts, or probabilistic execution. This may limit accuracy across diverse hardware workloads. Additionally, the PTU model does not yet capture noise, drift, or calibration overheads, which may impact performance and energy efficiency in real-world photonic systems. The learned cost models in TVM<sup>8</sup> were unsuitable due to their focus on ranking rather than physical simulation.

*b. Hardware Assumptions* LightCode leverages the structural property of Transformer models in which tensor products are not executed sequentially. This make it practical to use a fast, heuristic-based graph search by assuming non-contiguous photonic operations. However, for alternative model architectures or future hardware capable of accelerating a broader range of operations, this assumption may not hold, requiring a slower exhaustive search.

*c. Decoupled Selection and Scheduling* LightCode separates hardware selection from operation scheduling, which

can lead to suboptimal pipeline utilization. For example, selecting a busy photonic unit while the GPU is idle may increase overall makespan. A joint selection-scheduling strategy could improve performance.

*d. Limited Multi-Hardware Parallelism* Each Relay operation is assigned to a single hardware target, enabling task parallelism but restricting data parallelism. While LightCode manually enables photonic matmul tiling, automatic partitioning of operations across multiple hardware types (e.g., splitting a matmul across PTU and GPU) could reduce idle time and improve throughput.

## V. CONCLUSION

We present LightCode, a compiler optimization framework and hardware-aware simulator for mapping LLM inference workloads onto hybrid photonic-electronic architectures. As LLMs scale in size and usage, achieving low-latency, energy-efficient inference becomes increasingly critical. Photonic devices offer speed and energy advantages for the linear layers that dominate LLMs, but practical constraints necessitate heterogeneous deployments where photonics function as accelerators alongside GPUs. To address this challenge, LightCode introduces the Stacked Graph, a novel intermediate representation that encodes hardware-specific operation variants and inter-device transfer costs. Hardware mapping is framed as a constrained subgraph selection problem, enabling principled optimization of execution time and energy across heterogeneous systems. Simulations on GPT-2 and Llama-7B suggest that selective use of photonic accelerators for dense linear subgraphs yields significant energy savings. However, performance gains appear to depend on workload characteristics, hardware constraints, and optimization objectives—underscoring the need for a flexible, cost-aware compiler. Looking ahead, LightCode offers a modular platform for exploring compiler strategies at the intersection of machine learning and emerging hardware. Future extensions will integrate tighter scheduling, data-parallelism, and validation on photonic prototypes. By bridging compiler design and heterogeneous hardware, LightCode advances scalable, efficient LLM deployment on next-generation photonic hardware.

### A. Data Availability Statement

The data and analysis that support the findings of this study are openly available in the GitHub repository at <https://github.com/RyanTomich/LightCode>, reference commit 2b71d8a.

## VI. REFERENCES

<sup>1</sup>NVIDIA H100 Tensor Core GPU.

<sup>2</sup>ADC performance evolution: Walden figure-of-merit (FOM), August 2012.

<sup>3</sup>Martin Abadi, Paul Barham, Jianmin Chen, Zhifeng Chen, Andy Davis, Jeffrey Dean, Matthieu Devin, Sanjay Ghemawat, Geoffrey Irving, Michael

<sup>1</sup>Isard, Manjunath Kudlur, Josh Levenberg, Rajat Monga, Sherry Moore, Derek G. Murray, Benoit Steiner, Paul Tucker, Vijay Vasudevan, Pete Warden, Martin Wicke, Yuan Yu, and Xiaoqiang Zheng. TensorFlow: A system for large-scale machine learning, May 2016. arXiv:1605.08695 [cs].

<sup>4</sup>Maxwell G. Anderson, Shi-Yuan Ma, Tianyu Wang, Logan G. Wright, and Peter L. McMahon. Optical Transformers, February 2023. arXiv:2302.10360 [cs].

<sup>5</sup>Jason Ansel, Edward Yang, Horace He, Natalia Gimelshein, Animesh Jain, Michael Voznesensky, Bin Bao, Peter Bell, David Berard, Evgeni Burovski, Geeta Chauhan, Anjali Chourdia, Will Constable, Alban Desmaison, Zachary DeVito, Elias Ellison, Will Feng, Jiong Gong, Michael Gschwind, Brian Hirsh, Sherlock Huang, Kshiteej Kalambarkar, Laurent Kirsch, Michael Lazos, Mario Lezcano, Yanbo Liang, Jason Liang, Yinghai Lu, C. K. Luk, Bert Maher, Yunjie Pan, Christian Puhrsch, Matthias Reso, Mark Saroufim, Marcos Yukio Siraichi, Helen Suk, Shunting Zhang, Michael Suo, Phil Tillet, Xu Zhao, Eikan Wang, Keren Zhou, Richard Zou, Xiaodong Wang, Ajit Mathew, William Wen, Gregory Chanan, Peng Wu, and Soumith Chintala. PyTorch 2: Faster Machine Learning Through Dynamic Python Bytecode Transformation and Graph Compilation. In *Proceedings of the 29th ACM International Conference on Architectural Support for Programming Languages and Operating Systems, Volume 2*, pages 929–947, La Jolla CA USA, April 2024. ACM.

<sup>6</sup>Tom B. Brown, Benjamin Mann, Nick Ryder, Melanie Subbiah, Jared Kaplan, Prafulla Dhariwal, Arvind Neelakantan, Pranav Shyam, Girish Sastry, Amanda Askell, Sandhini Agarwal, Ariel Herbert-Voss, Gretchen Krueger, Tom Henighan, Rewon Child, Aditya Ramesh, Daniel M. Ziegler, Jeffrey Wu, Clemens Winter, Christopher Hesse, Mark Chen, Eric Sigler, Mateusz Litwin, Scott Gray, Benjamin Chess, Jack Clark, Christopher Berner, Sam McCandlish, Alec Radford, Ilya Sutskever, and Dario Amodei. Language Models are Few-Shot Learners, July 2020. arXiv:2005.14165 [cs].

<sup>7</sup>Pietro Caragiulo. pietro-caragiulo/survey-DAC, March 2024. original-date: 2020-03-24T17:13:22Z.

<sup>8</sup>Tianqi Chen, Thierry Moreau, Ziheng Jiang, Lianmin Zheng, Eddie Yan, Meghan Cowan, Haichen Shen, Leyuan Wang, Yuwei Hu, Luis Ceze, Carlos Guestrin, and Arvind Krishnamurthy. TVM: An Automated End-to-End Optimizing Compiler for Deep Learning. 2018.

<sup>9</sup>J. Feldmann, N. Youngblood, M. Karpov, H. Gehring, X. Li, M. Stappers, M. Le Gallo, X. Fu, A. Lukashchuk, A. S. Raja, J. Liu, C. D. Wright, A. Sebastian, T. J. Kippenberg, W. H. P. Pernice, and H. Bhaskaran. Parallel convolutional processing using an integrated photonic tensor core. *Nature*, 589(7840):52–58, January 2021. Publisher: Nature Publishing Group.

<sup>10</sup>Ryan Hamerly, Saumil Bandyopadhyay, and Dirk Englund. Asymptotically fault-tolerant programmable photonics. *Nature Communications*, 13(1):6831, November 2022. Publisher: Nature Publishing Group.

<sup>11</sup>Norman P. Jouppi, Cliff Young, Nishant Patil, David Patterson, Gaurav Agrawal, Raminder Bajwa, Sarah Bates, Suresh Bhatia, Nan Boden, Al Borchers, Rick Boyle, Pierre-luc Cantin, Clifford Chao, Chris Clark, Jeremy Coriell, Mike Daley, Matt Dau, Jeffrey Dean, Ben Gelb, Tara Vazir Ghaemmaghami, Rajendra Gottipati, William Gulland, Robert Hagmann, C. Richard Ho, Doug Hogberg, John Hu, Robert Hundt, Dan Hurt, Julian Ibarz, Aaron Jaffey, Alek Jaworski, Alexander Kaplan, Harshit Khaitan, Daniel Killebrew, Andy Koch, Naveen Kumar, Steve Lacy, James Laudon, James Law, Diemthu Le, Chris Leary, Zhuyuan Liu, Kyle Lucke, Alan Lundin, Gordon MacKean, Adriana Maggiore, Maire Mahony, Kieran Miller, Rahul Nagarajan, Ravi Narayanaswami, Ray Ni, Kathy Nix, Thomas Norrie, Mark Omernick, Narayana Penukonda, Andy Phelps, Jonathan Ross, Matt Ross, Amir Salek, Emad Samadiani, Chris Severn, Gregory Sizikov, Matthew Snelham, Jed Souter, Dan Steinberg, Andy Swing, Mercedes Tan, Gregory Thorson, Bo Tian, Horia Toma, Erick Tuttle, Vijay Vasudevan, Richard Walter, Walter Wang, Eric Wilcox, and Doe Hyun Yoon. In-Datacenter Performance Analysis of a Tensor Processing Unit. In *Proceedings of the 44th Annual International Symposium on Computer Architecture*, pages 1–12, Toronto ON Canada, June 2017. ACM.

<sup>12</sup>Jared Kaplan, Sam McCandlish, Tom Henighan, Tom B. Brown, Benjamin Chess, Rewon Child, Scott Gray, Alec Radford, Jeffrey Wu, and Dario Amodei. Scaling Laws for Neural Language Models, January 2020. arXiv:2001.08361 [cs].

<sup>13</sup>Samuel J Kaufman, Phitchaya Mangpo Phothilimthana, and Mike Burrows. Learned TPU Cost Model for XLA Tensor Programs. 2019.

<sup>14</sup>Chris Lattner, Mehdi Amini, Uday Bondhugula, Albert Cohen, Andy Davis, Jacques Pienaar, River Riddle, Tatiana Shpeisman, Nicolas Vasilache, and Oleksandr Zinenko. MLIR: A Compiler Infrastructure for the End of Moore’s Law, March 2020. arXiv:2002.11054 [cs].

<sup>15</sup>Kasper Groes Albin Ludvigsen. ChatGPT’s Electricity Consumption, March 2023.

<sup>16</sup>Boris Murmann. bmmurmann/ADC-survey, August 2024. original-date: 2022-12-25T18:23:24Z.

<sup>17</sup>Mitchell A. Nahmias, Thomas Ferreira de Lima, Alexander N. Tait, Hsuan-Tung Peng, Bhavin J. Shastri, and Paul R. Prucnal. Photonic Multiply-Accumulate Operations for Neural Networks. *IEEE Journal of Selected Topics in Quantum Electronics*, 26(1):1–18, January 2020.

<sup>18</sup>Soham Poddar, Paramita Koley, Janardan Misra, Niloy Ganguly, and Saptarshi Ghosh. Towards Sustainable NLP: Insights from Benchmarking Inference Energy in Large Language Models. In Luis Chiruzzo, Alan Ritter, and Lu Wang, editors, *Proceedings of the 2025 Conference of the Nations of the Americas Chapter of the Association for Computational Linguistics: Human Language Technologies (Volume 1: Long Papers)*, pages 12688–12704, Albuquerque, New Mexico, April 2025. Association for Computational Linguistics.

<sup>19</sup>Jared Roesch, Steven Lyubomirsky, Marisa Kirisame, Logan Weber, Josh Pollock, Luis Vega, Ziheng Jiang, Tianqi Chen, Thierry Moreau, and Zachary Tatlock. Relay: A High-Level Compiler for Deep Learning, August 2019. arXiv:1904.08368 [cs].

<sup>20</sup>Jared Roesch, Steven Lyubomirsky, Logan Weber, Josh Pollock, Marisa Kirisame, Tianqi Chen, and Zachary Tatlock. Relay: A New IR for Machine Learning Frameworks. In *Proceedings of the 2nd ACM SIGPLAN International Workshop on Machine Learning and Programming Languages*, pages 58–68, June 2018. arXiv:1810.00952 [cs].

<sup>21</sup>Nadav Rotem, Jordan Fix, Saleem Abdulrasool, Garret Catron, Summer Deng, Roman Dzhabarov, Nick Gibson, James Hegeman, Meghan Lele, Roman Levenstein, Jack Montgomery, Bert Maher, Satish Nadathur, Jakob Olesen, Jongsoo Park, Artem Rakhov, Misha Smelyanskiy, and Man Wang. Glow: Graph Lowering Compiler Techniques for Neural Networks, April 2019. arXiv:1805.00907 [cs].

<sup>22</sup>Siddharth Samsi, Dan Zhao, Joseph McDonald, Baolin Li, Adam Michaleas, Michael Jones, William Bergeron, Jeremy Kepner, Devesh Tiwari, and Vijay Gadepally. From Words to Watts: Benchmarking the Energy Costs of Large Language Model Inference. In *2023 IEEE High Performance Extreme Computing Conference (HPEC)*, pages 1–9, September 2023. ISSN: 2643-1971.

<sup>23</sup>Bhavin J. Shastri, Alexander N. Tait, T. Ferreira de Lima, Wolfram H. P. Pernice, Harish Bhaskaran, C. D. Wright, and Paul R. Prucnal. Photonics for artificial intelligence and neuromorphic computing. *Nature Photonics*, 15(2):102–114, February 2021. Publisher: Nature Publishing Group.

<sup>24</sup>John E. Stone, David Gohara, and Guochun Shi. OpenCL: A Parallel Programming Standard for Heterogeneous Computing Systems. *Computing in Science & Engineering*, 12(3):66–73, May 2010.

<sup>25</sup>Angelina R. Totović, George Dabos, Nikolaos Passalis, Anastasios Tefas, and Nikos Pleros. Femtojoule per MAC Neuromorphic Photonics: An Energy and Technology Roadmap. *IEEE Journal of Selected Topics in Quantum Electronics*, 26(5):1–15, September 2020.

<sup>26</sup>Ashish Vaswani, Noam Shazeer, Niki Parmar, Jakob Uszkoreit, Llion Jones, Aidan N Gomez, Łukasz Kaiser, and Illia Polosukhin. Attention is All you Need. In *Advances in Neural Information Processing Systems*, volume 30. Curran Associates, Inc., 2017.

<sup>27</sup>Thomas Wolf, Lysandre Debut, Victor Sanh, Julien Chaumond, Clement Delangue, Anthony Moi, Pierrick Cistac, Tim Rault, Rémi Louf, Morgan Funtowicz, Joe Davison, Sam Shleifer, Patrick von Platen, Clara Ma, Yacine Jernite, Julien Plu, Canwen Xu, Teven Le Scao, Sylvain Gugger, Mariama Drame, Quentin Lhoest, and Alexander M. Rush. HuggingFace’s Transformers: State-of-the-art Natural Language Processing, July 2020. arXiv:1910.03771 [cs].

<sup>28</sup>Zhizhen Zhong, Mingran Yang, Jay Lang, Christian Williams, Liam Kronman, Alexander Sludds, Homa Esfahanizadeh, Dirk Englund, and Manya Ghobadi. Lightning: A Reconfigurable Photonic-Electronic SmartNIC for Fast and Energy-Efficient Inference. In *Proceedings of the ACM SIGCOMM 2023 Conference*, pages 452–472, New York NY USA, September 2023. ACM.

<sup>29</sup>Wen Zhou, Bowei Dong, Nikolaos Farmakidis, Xuan Li, Nathan Youngblood, Kairan Huang, Yuhan He, C. David Wright, Wolfram H. P. Pernice, and Harish Bhaskaran. In-memory photonic dot-product engine with electrically programmable weight banks. *Nature Communications*, 14(1):2887, May 2023. Publisher: Nature Publishing Group.

## APPENDIX: SUPPLEMENTAL MATERIALS

### 1. Justification of the Tensor-Level Computation Graph

In conventional computing systems, an operation is typically defined at the assembly level specified by the ISA. However, this abstraction is ill-suited for multi-target compilation where various hardware may not agree on a single ISA. Moreover, attempting to partition instructions at the abstraction level of an ISA across heterogeneous devices complicates issues such as memory access, register synchronization, and control flow management.

LightCode adopt a higher-level abstraction aligned with the TVM<sup>8</sup> compiler framework: we define an operation as a function that consumes and produces tensor data, as in the TVM Relay IR<sup>19,20</sup>. Under this model, a computation graph represents the dataflow dependencies between tensor operations, such as matrix multiplications, element-wise activations, and normalization layers. Each node in the computation graph is parameterized by input tensor shapes, the operation performed, and the resulting output shapes. These parameters allow the compiler to reason about hardware feasibility, instruction count, data movement costs, and parallelization opportunities. This tensor-centric representation provides a more flexible and hardware-agnostic foundation for compiler optimizations. It enables operations to be scheduled across hardware targets while maintaining functional correctness. This graph structure defines the search space for optimizations, particularly for mapping key primitives—such as tensor products—to specialized accelerators.

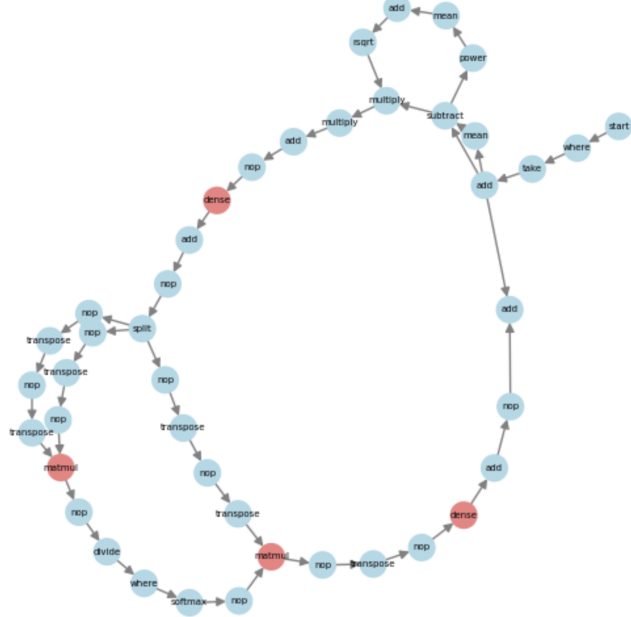


FIG. 7. Example partition 1 of the GPT-2 Small Transformer in Relay IR. A subset of the computation graph is shown after partitioning. Highlighted nodes are mapped to PTU.

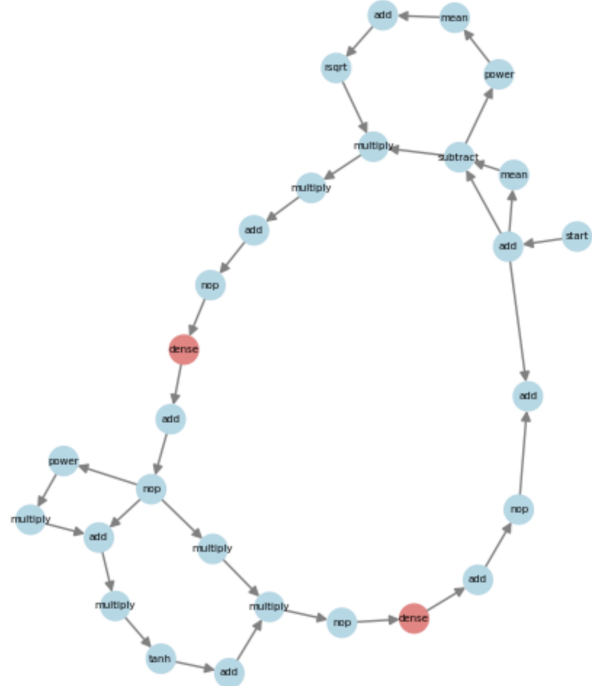


FIG. 8. Example partition 2 of the GPT-2 Small Transformer in Relay IR. A subset of the computation graph is shown after partitioning. Highlighted nodes are mapped to PTU.